2012 IEEE/RSJ International Conference on
Intelligent Robots and Systems
October 7-12, 2012. Vilamoura, Algarve, Portugal

Improved Grasp Robustness through Variable Transmission Ratios in Underactuated Fingers

Stefan A.J. Spanjer, Ravi Balasubramanian, *Member, IEEE,* Just L. Herder, *Member, IEEE,* and Aaron M. Dollar, *Member, IEEE*

***Abstract*— This paper investigates the possibility of increasing the robustness of underactuated grasping through the use of variable transmission ratios. We propose a 4-step procedure to investigate and improve the robustness of an underactuated finger on a fixed object. This procedure maximizes the robustness against random force disturbances to the maximum obtainable value under given circumstances. A simulation study is presented that analyzes the disturbance robustness, followed by an experimental study to confirm the effect. The variable transmission ratio is a promising means to increase grasp robustness and has great application potential.**

I. Introduction

ADAPTIVE underactuation has been utilized extensively in the design of robotic hands in order to allow for high degree-of-freedom, yet lightweight and compact systems (e.g. [1-4]). Benefits of this approach include passive adaptability to a wide range of object size and shape, lower contact forces during object acquisition, mechanical simplicity and durability, and lack of need for complex sensing and control. However, one of the disadvantages to the approach comes during precision grasping, where unconstrained DOFs can cause the mechanisms to reconfigure and potentially lose the grasp. Power grasps, where the hand envelopes the object, are more robust than precision grasps, where the object is grasped between the tips of the fingers. Precision grasps are necessary when objects are small or when objects are approached from above.

There are several factors that influence the stability of an underactuated finger's precision grasp, including the object-finger contact location, the friction parameters, the finger configuration, and the mechanism design parameters. Specifically, equilibrium occurs when the 'equilibrium point' of the finger's distal link is contained within or on the edge of the friction cone (Fig. 1A). Otherwise, the finger will slide [2].

A few previous studies have investigated stability. The stability of a finger in different control modes and different underactuation mechanism configurations was investigated in depth in [5]. In [6], the stability of precision grasps was increased by modifying the curvature of the distal phalanx, the application of a mechanical limit and the application of a compliant joint. Other work has investigated friction-based coupling mechanisms as a means to remove the remnant degrees of freedom for precision grasps [7]. This approach uses a pulley that prevents rotation after a certain preload has been overcome, removing a DOF from the system.

The goal of this paper is to present an alternative way to improve the robustness of a precision grasp. We propose a method of mechanically varying the transmission ratio between the proximal and distal joints of a two-link underactuated finger after establishing contact with the object (Fig. 1B). By changing the radius of the proximal pulley after grasping, the equilibrium point can be controllably shifted from the edge of the friction cone to the center of the cone. By doing so, the robustness against random force disturbances is maximized and the required friction force in the newly established configuration goes to zero.

The structure of the paper is as follows. In section II we describe the method and model used to set up a 4-step procedure to investigate and improve the robustness of an

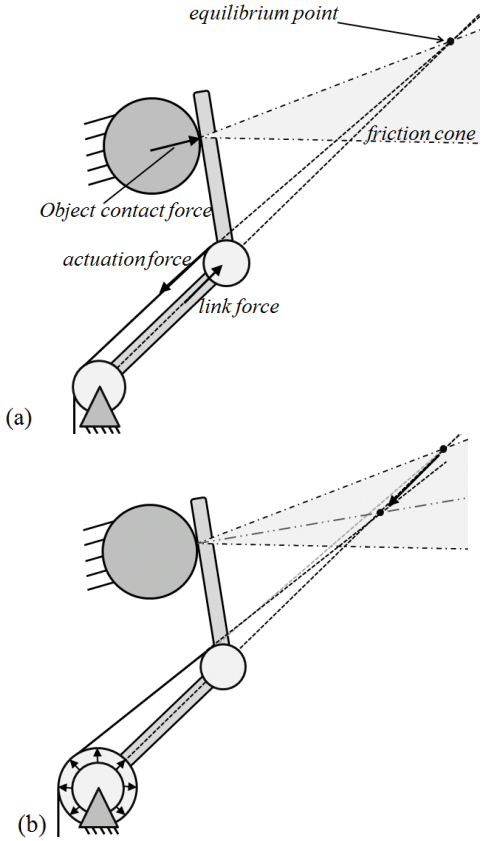

Fig. 1: Relocation of equilibrium point in center of friction cone

S.A.J. Spanjer and J.L. Herder are with the Laboratory of Mechanical Automation and Mechatronics, Faculty of Engineering Technology, University of Twente, Enschede, Netherlands (e-mail: s.a.j.spanjer@alumnus.utwente.nl, j.l.herder@utwente.nl).
R. Balasubramanian and A.M. Dollar are with the Department of Mechanical Engineering and Materials Science, School of Engineering and Applied Science, Yale University, New Haven, CT USA (e-mail: ravi.balasubramanian@yale.edu, aaron.dollar@yale.edu).

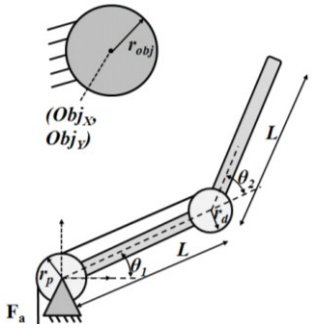

Fig. 2: Different parameters

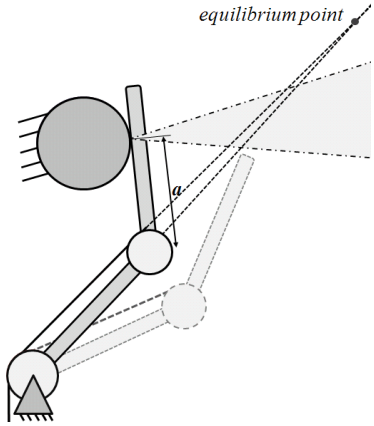

Fig. 3: Step 1, making contact with object

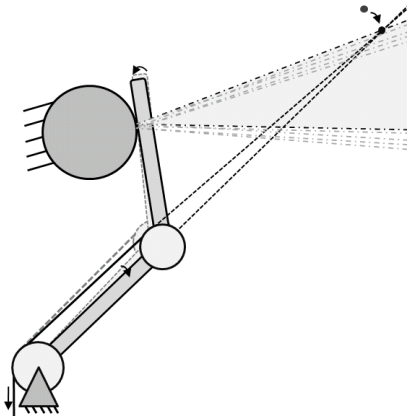
Fig. 4: Step 3, reconfiguration

underactuated finger on a fixed object. In section III we present the results of a simulation study in which the mechanical parameters of the finger and coupling mechanisms are varied in order to evaluate their effect on performance. In section III we also validate the model by an experiment and show that the robustness increases by varying the transmission ratio. Finally the discussion and conclusions follow in sections IV and V respectively.

II. Underactuated Precision Grasp Model

We propose a 4-step procedure to investigate and improve the robustness of an underactuated finger with 2 phalanges that grasps a fixed object. In step 1 of this procedure it is determined where the finger contacts an object. In step 2 the equilibrium of the finger is checked. In step 3 the finger slides along the object in case there is no equilibrium. We assume quasi-static conditions and equal coefficients of static and kinetic friction. The sliding will result in equilibrium or in contact loss of the object. In case of equilibrium, step 4 describes how the robustness of this equilibrium will be improved. After the 4-step procedure the consequences of an external disturbance force acting on the distal link are investigated. This procedure is valid for underactuated fingers of any architecture. In this paper we develop a 2D model for a two-phalange finger based on a cable-pulley system for practical reasons. We will assume circular rigid objects.

A. Introduction of the Equilibrium Point

In Fig. 1A the intersection of the action lines of the actuation force and link force is called the equilibrium point. This point is equal to the instantaneous center of rotation of the distal link in case the actuation cable is fixed and there is no contact with an object, because then the system behaves as a four bar mechanism and the distal link rotates about this point.

An underactuated finger that contacts a fixed object by its distal phalanx (precision grasp) is only in equilibrium if the action line of the contact force intersects the equilibrium point, because equilibrium of three forces is only possible when the three forces intersect at one point. The distal link rotates clockwise if the object force produces a clockwise moment about the equilibrium point and counterclockwise in the other case. In both cases sliding occurs and this results in contact loss with the object or in a new state of equilibrium if the action lines of the three forces intersect at one point. When friction is taken into account, the same theory is valid, but now the equilibrium point must be inside or on the edge of the friction cone (Fig. 1A). The projection of the equilibrium point on the distal link is often also called the equilibrium point [2]. In this paper the projection is called the projected equilibrium point.

B. Underactuated Finger Model

The finger is actuated by a tendon with force F_a and the finger has pulleys with radii r_p and r_d and angular spring stiffnesses K_p and K_d at the proximal and distal joint, respectively. In Fig. 2 the various parameters are shown. Both links have length L and width d, the proximal link is rotated with angle θ_1 with respect to the horizontal. The distal link is rotated with angle θ_2 with respect to the proximal link. In the analysis the finger contacts a fixed circular object at position (Obj_x, Obj_y) with radius r_{obj}.

TABLE I
NOMENCLATURE

parameter	*definition*
θ_1, θ_2	deflected angle
$\theta_{1,ini}, \theta_{2,ini}$	spring rest angle
$\delta\theta_1, \delta\theta_2$	additional angle change to make contact with object
$\Delta\theta_1, \Delta\theta_2$	angle change when finger slides
r_p, r_d	proximal and distal pulley radii
K_p, K_d	proximal and distal joint stiffnesses
F_a	actuation force
F_n	normal contact force
F_t	tangential contact force
$F_{a,ini}$	required actuation force to move finger to object
F_e	External disturbance force that applies on the distal link
ΔF_a	increment of the actuation force
$\Delta F_n, \Delta F_t$	increments of the normal and tangential contact force
$F_{n,ini}, F_{t,ini}$	normal and tangential contact force before F_e applies
L	proximal and distal link length
d	proximal and distal link thickness
a	distance from distal joint to contact point
μ	coefficient of friction
r_{obj}	radius of the object
(Obj_x, Obj_y)	position of the object

C. Procedure to analyze grasping behavior and improve robustness

1) Step 1: Contacting the Object

In step 1 the finger moves from its rest position with angles $\theta_{1,ini}$ and $\theta_{2,ini}$ to a first contact position where it touches the object (Fig. 3). In this position the normal contact force F_n and the tangential friction force F_t exerted by the object on the distal phalanx are zero, so the actuation force $F_{a,ini}$ is just high enough to overcome the spring forces. The contact force location on the distal link named a and the angle changes $\delta\theta_1$and $\delta\theta_2$ depend on the ratio of the spring stiffnesses and pulley radii. With the following equations the variables $a, \delta\theta_1$and $\delta\theta_2$ are calculated:

$$\delta\theta_1 - \delta\theta_2 \frac{K_d}{K_p}\frac{r_p}{r_d} = 0 \tag{1}$$

$$L\begin{Bmatrix}\cos(\theta_{1,ini}+\delta\theta_1)\\ \sin(\theta_{1,ini}+\delta\theta_1)\end{Bmatrix} + a\begin{Bmatrix}\cos(\theta_{12,ini}+\delta\theta_{12})\\ \sin(\theta_{12,ini}+\delta\theta_{12})\end{Bmatrix} - (r_{obj}+d)\begin{Bmatrix}\cos(\theta_{12,ini}+\delta\theta_{12}-\pi/2)\\ \sin(\theta_{12,ini}+\delta\theta_{12}-\pi/2)\end{Bmatrix} - \begin{Bmatrix}Obj_x\\ Obj_y\end{Bmatrix} = \mathbf{0} \tag{2}$$

where $\theta_{12,ini} = \theta_{1,ini} + \theta_{2,ini}$ and $\delta\theta_{12} = \delta\theta_1 + \delta\theta_2$. Subsequently $F_{a_{ini}}$ is calculated: $F_{a_{ini}} = K_{11}\delta\theta 1/r1$.

2) Step 2: Equilibrium Check

Step 2 investigates if the finger is in equilibrium. An increase of the actuation force results in contact force F_n and friction force F_t exerted by the object on the distal link. The corresponding equations are:

$$-\boldsymbol{J_n^T}\begin{Bmatrix}0\\ F_n\end{Bmatrix} - \boldsymbol{K\delta\theta} + \boldsymbol{J_a^T}F_a + \boldsymbol{J_t^T}F_t = \mathbf{0} \tag{3}$$

where $\boldsymbol{K} = diag(K_p, K_d)$ is the stiffness matrix, $\boldsymbol{J_a} = (r_p, r_d)$ represents the actuator Jacobian and $\boldsymbol{J_t} = (L_1 \sin\theta_2 - d, -d)^T$ transfers the friction force to joint torques. F_a is equal to the sum of $F_{a_{ini}}$ and an additional force ΔF_a. Otherwise F_n and F_t are equal to zero, because $F_{a_{ini}}$ is the required force to move the finger in free space, see Step 1. The matrix $\boldsymbol{J_n}$ maps the contact force to joint torques [2]:

$$\boldsymbol{J_n} = \begin{bmatrix}0 & 0\\ a + L\cos\theta_2 & a\end{bmatrix} \tag{4}$$

There is only equilibrium if the friction force is located inside or on the edge of the friction cone: $-\mu F_n \le F_t \le \mu F_n$, where μ is the coefficient of friction. Substituting the results of (3) results in the following equilibrium conditions:

$$-\mu \le \frac{r_d - r_p + r_d\frac{L}{a}\cos\theta_2}{r_d\frac{L}{a}\sin\theta_2 + \frac{d}{a}\left(r_p - r_d\left(1 + \frac{L}{a}\cos\theta_2 + \frac{1}{a}\right)\right)} \le \mu \tag{5}$$

Another way to check equilibrium is by using the equilibrium point. If this point is located in or on the friction cone, then there is equilibrium. If it is outside the friction cone, then sliding will occur. Both approaches have the same result.

3) Step 3: Sliding of the Finger

Step 3 investigates the sliding of the finger along the object by a quasi-static approach, as in [5]. It is assumed that there is no initial equilibrium. The same equilibrium equations as in (3) are used, but now F_n, F_a, F_t and $\boldsymbol{\delta\theta}$ are replaced by ΔF_n, ΔF_a, ΔF_t and $\boldsymbol{\Delta\theta}$. These variables represent the additional forces and configuration change on top of the force and configuration state that were achieved in Step 1. Since there is sliding, $\Delta F_t = \mu\Delta F_n$. In this situation F_t points upwards, μ equals $-\mu$ when the finger slides in the opposite direction. At the first iteration $\theta_2 = \theta_{2,ini} + \delta\theta_2$ is updated in $\boldsymbol{J_c}$ and $\boldsymbol{J_f}$. Together with the equilibrium equations two contact constraints are used to describe the contact with the object. These constraints are defined as follows:

$$-\Delta a - \frac{\Delta\theta_1(r_{obj}+d)L\cos(\theta_2)}{a} - \Delta\theta_1 L\sin(\theta_2) = 0 \tag{6}$$

$$-\Delta\theta_2 - \frac{\Delta\theta_1 L\cos(\theta_2)}{a} - \Delta\theta_1 = 0 \tag{7}$$

Δa is the change of the normal force contact position on the distal link. ΔF_a is a small value from which $\Delta\theta_1, \Delta\theta_2, \Delta a$ and ΔF_n are calculated at every iteration. After every iteration the increments $\Delta\theta_1, \Delta\theta_2, \Delta a$ and ΔF_c are added to the total θ_1, θ_2, a, F_c and $\boldsymbol{J_c}$ and $\boldsymbol{J_f}$ are updated. For accuracy ΔF_a must be small, such that $\Delta\theta_1, \Delta\theta_2, \Delta a$ are small too. The iterative procedure is stopped when contact is lost or $\Delta\theta_1$ and $\Delta\theta_2$ are very small. In the last case the force lines intersect in one point (the equilibrium point) and further increase of the actuation force results only in an increase of the contact force and friction force. Contact loss occurs through clockwise or counterclockwise rotation of the distal phalanx, depending on the variables.

The equilibrium point also provides information concerning the sliding of the finger. The finger achieves a state of equilibrium if the equilibrium point reaches the boundary of the friction cone (Fig. 4).

4) Step 4: Change of the Transmission Ratio

This step assumes that the finger achieves a state of equilibrium. Due to a maximized friction force, the achieved state of equilibrium is not very robust. Even a small disturbance force pointing in the opposite direction of the friction force is enough to break equilibrium. Therefore, it is better to reduce the friction force to zero in order to minimize the chance that a disturbance force in any direction will break equilibrium. By changing the radius of the proximal pulley the equilibrium point is shifted from the edge of the cone to the center and so a zero friction force is required to maintain equilibrium. The consequences of a

radius change for the equilibrium are calculated by applying the quasi-static procedure again, but now ΔF_t is a variable and not equal to $\mu\Delta F_n$ and $\boldsymbol{J_a} = (\Delta r_p, 0)$. F_a is held constant. There are five variables (Δa, $\Delta\theta_1$, $\Delta\theta_2$, ΔF_n and ΔF_t) but only four equations. Solving for the variables in terms of Δa, it can be shown that the only solution that exist is for no configuration change ($\Delta a = 0$). The total required radius change to decrease the friction force to zero is calculated as follows:

$$\Delta r_p = \left(\frac{d}{a} L\cos\theta_2 + L\sin\theta_2\right)\frac{F_t}{F_a} \tag{8}$$

ΔF_n is equal to:

$$\Delta F_n = \frac{\frac{d}{a}\Delta r_p F_a}{\frac{d}{a} L\cos\theta_2 + L\sin\theta_2} \tag{9}$$

The equilibrium point also provides information concerning the robustness of the equilibrium. By changing the radius of the proximal pulley the equilibrium point shifts along the imaginary extended line through the proximal phalanx, see Fig. 1B. In order to shift this point to the center of the cone for maximal robustness Δr_p is equal to:

$$\Delta r_p = r_d\left[\frac{L}{a}\cos\theta_2 - \frac{L}{a + d\mu}\frac{\sin\left(\frac{\pi}{2} - \theta_2 - \operatorname{atan}\mu\right)}{\sin\left(\frac{\pi}{2} + \operatorname{atan}\mu\right)}\right] \tag{10}$$

This radius change derived from trigonometry is exactly the same as the radius change calculated in (8). In case the friction force points to the other direction, μ is negative.

D. Effect of Disturbance Force

This section investigates how the finger reacts on external disturbances after grasping an object. Thereby it is not assumed that the transmission ratio is changed to improve the robustness. The external disturbance force F_e applies on the distal phalanx at position b under angle γ (Fig. 5). The actuation force is held constant and it is assumed that there is no reconfiguration. The following equations are used to calculate ΔF_n and ΔF_t that are needed on top of the normal and friction forces to hold equilibrium:

$$-\boldsymbol{J_n^T}\begin{Bmatrix}0\\ \Delta F_n\end{Bmatrix} + \boldsymbol{J_t^T}\Delta F_t + \boldsymbol{J_e^T}\begin{Bmatrix}\sin\gamma\\ \cos\gamma\end{Bmatrix}F_e = \boldsymbol{0} \tag{11}$$

where $\boldsymbol{J_n}$ and $\boldsymbol{J_t}$ are similar to $\boldsymbol{J_n}$ and $\boldsymbol{J_t}$ in (3). The matrix $\boldsymbol{J_e}$ maps the external force to joint torques:

$$\boldsymbol{J_e} = \begin{bmatrix} d + L\sin\theta_2 & b + L\cos\theta_2 \\ d & b\end{bmatrix} \tag{12}$$

From (11) ΔF_n and ΔF_t are calculated. It must be checked if $-\mu(F_{n,ini} + \Delta F_n) \le F_{t,ini} + \Delta F_t \le \mu(F_{n,ini} + \Delta F_n)$, where $F_{t,ini}$ and $F_{n,ini}$ are the friction and contact force before the external force applies and ΔF_n and ΔF_t are substituted:

$$\begin{aligned}&-\mu\left(\frac{a}{b} + \frac{a\cos\gamma\tan\theta_2 + \frac{a}{b}d(\cos\gamma + 2\sin\gamma\tan\theta_2)}{a\tan\theta_2 + d}\frac{F_e}{F_{n,ini}}\right)\\ &\le \frac{F_{t,ini}}{F_{n,ini}}\frac{a}{b} + \left[\left(1 - \frac{a}{b}\right)\frac{\cos\gamma}{\tan\theta_2 + \frac{d}{a}} - \sin\gamma\frac{a}{b}\frac{\tan\theta_2 - \frac{d}{a}}{\tan\theta_2 + \frac{d}{a}}\right]\frac{F_e}{F_{n,ini}}\\ &\le \mu\left(\frac{a}{b} + \frac{a\cos\gamma\tan\theta_2 + \frac{a}{b}d(\cos\gamma + 2\sin\gamma\tan\theta_2)}{a\tan\theta_2 + d}\frac{F_e}{F_{n,ini}}\right)\end{aligned} \tag{13}$$

In case the proximal pulley radius is changed in step 4, $F_{t,ini}$ is equal to zero.

III. Results

A. Simulation Studies

In this section, the model used to study how the range of required transmission ratio changes for different kinematic configurations is simulated as well as the robustness against external disturbance forces after changing the transmission ratio. The parameters held constant in those 2 studies are $L = 0.1\,m$, $r_d = 0.01\,m$, $\mu = 0.3$, $\theta_{1,ini} = 0.44\,rad$ (25°), $\theta_{2,ini} = 0.79\,rad$(45°), $K_p = 0.001\,Nm/rad$ and $K_d = 0.005\,Nm/rad$. For simplicity, the links have zero width ($d = 0$).

1) Required Transmission Ratio Change

Fig. 6 shows how the required joint coupling ratio change, $\Delta r_p/r_p$, varies as a function of θ_2. For a given transmission ratio and θ_2, it tells how large $\Delta r_p/r_p$ must be in order to move the equilibrium point from the boundary to the center of the friction cone, maximizing the robustness to a randomly distributed disturbance force. It is clear that $\Delta r_p/r_p$ increases when θ_2 increases. When θ_2 is larger, the equilibrium point has to shift more in order to reach the center of the cone. $\Delta r_p/r_p$ increases asymptotically, and this asymptote is located at $\theta_2 = \pi/2 - \operatorname{atan}\mu$. At this point the

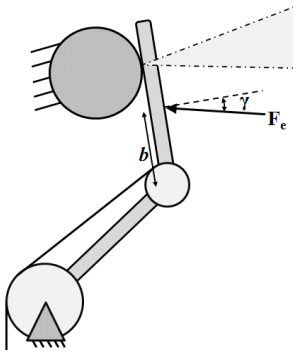

Fig. 5: External disturbance force acting on the distal link

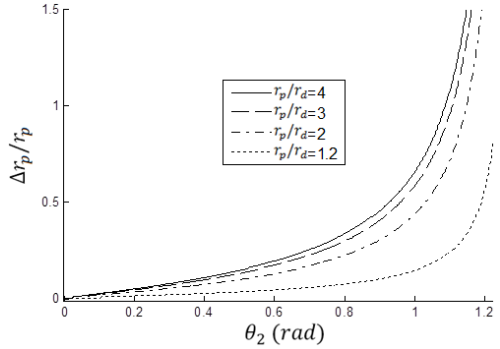

Fig. 6: $\Delta r_p/r_p$ as a function of θ_2 and different transmission ratios

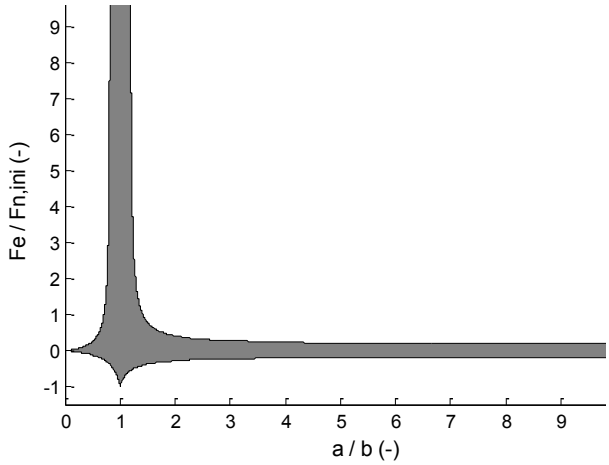

Fig. 7: Robustness diagram ($\gamma = 0°$, eq. point in center of cone)

object is located at the distal joint, so $a/L = 0$ and the upper boundary of the friction cone is parallel to the proximal link. As a consequence, the equilibrium point will always be located on the upper boundary for every radius change.

The required radius change increases when the coefficient of friction increases. because the equilibrium point has to shift more in order to reach the center of the cone.

2) Robustness to external forces

Fig. 7 shows the allowable disturbance force F_e normalized by the initial normal contact force $F_{n,ini}$, as a function of the ratio between the contact position a and the disturbance force location b. In this case the robustness is already improved by changing the transmission ratio. The disturbance force applies normal to the link ($\gamma = 0\,rad$) and $\theta_2 = \pi/6\,rad$. Grey areas under the curve are stable regions, and white areas outside the curves are unstable regions. It is clear from Fig. 7 that for a disturbance force pointing towards the object a stable region exists around $a/b = 1$, with vertical asymptotes at:

$$1 - \mu \tan\theta_2 \leq \frac{a}{b} \leq 1 + \mu \tan\theta_2 \qquad (14)$$

This is expected, because a larger disturbance force results in a larger normal contact force, so the normal friction force can also be larger.

The equilibrium breaks for $a/b = 1$ and $F_e/F_{n,ini} < -1$, because in this case the disturbance force pulls the finger away from the object, so if this external force is larger than the initial contact force, there will be loss of contact.

For a disturbance force applied tangential to the link ($\gamma = \pi/2\,rad$), the stable area has lower and upper boundaries at $-\mu$ and μ. If the robustness is not improved by changing the transmission ratio, then the equilibrium point is located on the edge of the cone, and then the lower and upper boundaries of the stable area are shifted μ.

B. Experimental Studies

In order to evaluate these concepts in a real-world scenario, an experimental setup was developed to allow for active changes in the coupling ratio as well as the measurement of contact forces on a target object. With this

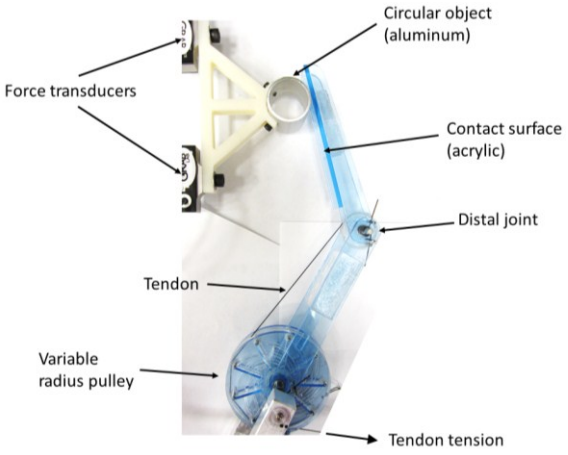

Fig. 8: Experiment set up

setup, we verify that the friction force at the contact location decreases towards zero when the radius of the proximal pulley is changed to move the equilibrium point towards the center of the friction cone.

Fig. 8 shows the setup of the experiment, including an acrylic finger with music-wire springs and low-friction joints, a small cylindrical object mounted to a 2-DOF force-sensing platform (using two 1-DOF load cells, Transducer Techniques MLP-10), and a torque-controlled motor (Maxon F2140) applying the tendon-based actuation. The joint rest angles and stiffnesses are the same as in the simulation described above.

The proximal pulley employs a mechanism that allows the effective radius to be changed by rotating a top and bottom plate with respect to one another (Fig. 9). Shafts around which the tendon is routed (i.e. the effective pulley) are located between the straight slots in the bottom plate and the curved slots in the top plate. As the plates rotate with respect to one another, the shafts move radially, changing the effective pulley radius. Small pulleys are mounted on the shafts. The logarithmic spiral slots are designed to have a relatively large angle with the radial slots in order to reduce friction and allow smooth movement of the pins. The whole system is connected to the proximal shaft with bearings, so it can rotate freely.

The experiment is executed as follows. The finger is initially at rest, $\theta_{1,ini}$ and $\theta_{2,ini}$, and the actuation force is smoothly increased to 12 N. During this motion, the finger makes contact with the object and slides until the equilibrium point reaches the edge of the friction cone, after which no additional movement can occur. Next the angles $\theta_1$and θ_2 are measured and the contact and friction force are

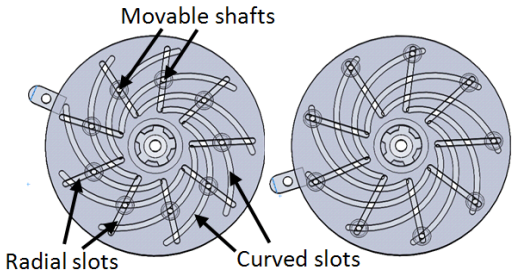

Fig. 9: Variable radius

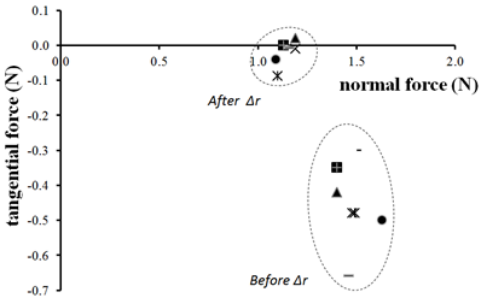

Fig. 10: Contact forces before and after proximal radius change

calculated from the sensors. With this data the required radius change is calculated from (8). The proximal pulley radius is changed manually to the desired new radius, and the contact and friction force are measured again. During the radius change we ensure that no contact/kinematic changes occur.

Fig. 10 shows the results from this study. The normal contact force is presented on the x-axis and the tangential friction force on the y-axis. Each symbol type represents a different trial, for each trial the object position and radius are the same. The points clustered in the lower right part of the figure are the measured forces before the radius is changed, while the points on the upper left part of the figure represent the forces after the radius is changed. From Fig. 10 it is clear that the friction force decreases towards zero when the radius is changed. Since the contact location did not also change, this result indicates that we are able to successfully move the equilibrium point into the center of the friction cone, thereby increasing the amount of allowable disturbance force before the grasp is destabilized.

IV. Discussion

In this paper we have suggested a way to improve robustness of underactuated precision grasps using a variable coupling ratio implemented through a changeable pulley radius and showed a successful experimental implementation of the concept. While the specific implementation of the concept was through a pulley tendon mechanism, the theory holds for linkage-based transmissions, in which one of the bars has variable length such as through a slider mechanism.

An assumption of the model is the 2D assumption. The friction cone is assumed to be 2D, but is in fact 3D. If in a grasp the equilibrium point is located on the edge of the 2D friction cone, then there is no out-of-plane friction force left for out-of-plane forces, for example gravity forces. If the equilibrium point is located in the center of the 2D cone, then out-of-plane forces can be compensated by an out-of-plane friction force.

In general, directions and contact points of disturbances are not known, so by bringing the friction force to zero a general higher robustness is achieved. However, if the possible disturbance forces are known ahead of time, then the radius can be changed such that the robustness maximizes with respect to this disturbance. For example if a disturbance force acts along the distal link in a certain direction, then the equilibrium point can be moved to the side of the friction cone such that the maximal allowable tangential force can be doubled.

The object is assumed to be fixed in the model. The equilibrium of the object is not considered. Depending on the number of contact points between object and fingers, a change of the transmission ratio of one finger could result in shifting of the object with respect to the fingers.

The option to change the proximal pulley radius introduces an additional degree of freedom, and currently we add another actuator to control this degree of freedom. The degree of underactuation of the system therefore remains constant. The advantage of this approach with respect to fully actuated fingers is that the adaptability behavior is preserved, which makes it easier to pick up different objects.

V. Conclusion

In this paper we proposed a 4-step procedure to analyze and increase the robustness of a precision grasp. This procedure maximizes the robustness against random force disturbances to the maximum obtainable value under given circumstances. The robustness is increased by relocating the equilibrium point into the center of the friction cone by applying variable transmission ratio between the proximal and distal link. This is verified with an experiment. The 4-step procedure is valid and is applicable to other types of underactuated fingers, for example four bar mechanisms. The variable transmission ratio maximizes the robustness, from 0 to μF_n. In the specific case of the pulley-cable mechanism studied in this paper the normal contact force is linearly related to the actuation force, so the allowable disturbance force can be higher when the actuation force is increased. A robustness diagram was proposed that shows which disturbance forces and locations can be rejected by the finger. Compared to other methods to improve robustness of precision grasps, this method takes maximum advantage of friction between object and finger and improves the robustness after the object has been grasped.

References

[1] S. Hirose and Y. Umetani. The development of soft gripper for the versatile robot hand. *Mechanism and Machine Theory,*, 13:351–359, 1978.

[2] L. Birglen, T. Laliberté, and C. Gosselin. *Underactuated Robotic Hands*. Springer, 2008.

[3] A. M. Dollar and R. D. Howe. The Highly Adaptive SDM Hand: Design and Performance Evaluation, *International Journal of Robotics Research*, vol. 29(5), pp. 585–597, 2010.

[4] C. Meijneke, G. A. Kragten, and M. Wisse, "Design and performance assessment of an underactuated hand for industrial applications," *IFToMM/ASME International Workshop on Underactuated Grasping*. pp. 9-15, 2011.

[5] R. Balasubramanian, J.T. Belter, A.M. Dollar. "Disturbance Response of Two-link Underactuated Serial-link Chains", *JMR*, 2011,??

[6] G. A. Kragten, M. Baril, C. Gosselin, J. L. Herder, "Stable Precision Grasps by Underactuated Fingers". *IEEE Transactions on Robotics*, vol. 27, no. 6, Dec. 2011.

[7] J.T. Belter and A.M. Dollar, "Underactuated Grasp Acquisition and Stability using Friction Based Coupling Mechanisms," proceedings of the 2011 IEEE International Conference on Robotics and Automation (ICRA), Shanghai, China, May 9-13, 2011.